



COMPUTATIONAL SIMULATION OF A LOW-DISPLACEMENT MOTORCYCLE SI ENGINE OPERATING WITH GASOLINE AND ETHANOL BLENDS

Rubelmar Maia de Azevedo Cruz Neto

rubelmar.neto@gmail.com

Albino José Kalab Leiroz

leiroz@mecanica.coppe.ufrj.br

Manuel Ernani de Carvalho Cruz

manuel@mecanica.coppe.ufrj.br

Universidade Federal do Rio de Janeiro – COPPE/UFRJ

Caixa Postal 68503, CT, Cidade Universitária, Rio de Janeiro, RJ, 21941-972, Brasil

Abstract. *In the present work, results from numerical simulations of a low-displacement motorcycle SI engine operating with gasoline and ethanol blends using the commercial code AVL Boost™ are discussed. The simulations and energy analysis are conducted considering the motorcycle engine operating in the range 4500-8500 rpm. The results obtained show that an increase in the ethanol content in the fuel blend causes an increase in the energy efficiency of the engine. It is also observed that an increase in the engine speed causes a decrease in the energy efficiency.*

Keywords: *engine simulation, motorcycle, gasoline, ethanol, flex-fuel*

1. INTRODUCTION

Brazil holds a wide experience with alternative and renewable fuels. The consolidated use of ethanol as an alternative to gasoline, and the development and utilization of biodiesel place the country experience in this field as a recognized worldwide reference. As a matter of fact, in 2003, the assembly of automotive vehicles with the flex-fuel technology started in Brazil, giving the customer the option to use gasoline and ethanol together in any proportion.

After a recent significant growth of the motorcycle sales in the Brazilian market, and following a national tendency, the motorcycle makers invested in the development of the flex-fuel technology for low-displacement SI engines. In 2009 the first commercial flex-fuel motorcycle in the world was assembled in Brazil.

While environmental pollution becomes a more serious issue, the regulations to limit pollutant emissions from light automotive vehicles get increasingly more rigorous worldwide. As the motorcycles increase their share in the national fleet, and because their emissions are high due to outdated technology employed by the manufacturers in Brazil, the Federal Government decided to act upon this segment as well. Based on the European experience, the Brazilian Federal Government passed the Resolution CONAMA no. 297/02, thereby creating the Program for Control of Air Pollution by Motorcycles and Similar Vehicles – PROMOT, imposing limits on pollutant emissions by motorcycles and similar vehicles (Vicentini, 2011).

It is thus apparent that the computational simulation of motorcycle SI engines is of great practical interest. The aim is to develop more efficient engines that consume less fuel and emit less gaseous pollutants without compromising performance. Besides, computational simulation provides input data for exergetic analysis of engine cycles (Azevedo Cruz Neto, 2013; Carvalho *et al.*, 2013).

The present work fits in this context, with the objective to computationally simulate a low-displacement motorcycle SI engine operating with gasoline and ethanol blends over a chosen range of engine speeds. Here, the engine is modeled with the aid of the commercial engine simulator AVL Boost™.

2. ENGINE SIMULATION MODELS

The engine simulator AVL Boost™ makes available several different models for combustion and heat transfer phenomena. The software has been successfully used in engine simulations in Brazil (Carvalho *et al.*, 2013; Azevedo Cruz Neto, 2013; Melo, 2012; Carvalho *et al.*, 2010) as well as in research works abroad (Cordtz *et al.*, 2011; Teng, 2011; Tuan *et al.*, 2011).

The simulator AVL Boost™ is able to calculate the variations of the thermodynamic properties cycle-by-cycle or, in one cycle, as functions of the crankshaft angle (AVL, 2011a). Depending on the choice of the combustion model, a zero-dimensional or a quasi-dimensional simulation is carried out. The engine is modeled through its components or parts, such as *ducts, connections, air filter, catalyst, cylinder*, among others, that possess a set of geometrical and physical properties. Fig. 1 represents schematically the energy balance in the engine cylinder.

The calculation of the internal thermal energy variation in the cylinder as a function of the crankshaft angle, $d(m_{mixt}u)/d\theta$, is given by the first law of thermodynamics, expressed by (AVL, 2011a)

$$\frac{d(m_{mixt}u)}{d\theta} = -P \frac{dV}{d\theta} + \frac{\partial Q_{comb}}{\partial \theta} - \sum \frac{\partial Q_w}{\partial \theta} + \sum \frac{dm_i}{d\theta} \times h_i - \sum \frac{dm_e}{d\theta} \times h_e - h_{bb} \frac{dm_{bb}}{d\theta} - q_{vap} f \frac{dm_{vap}}{d\theta} \quad (1)$$

where $-P dV/d\theta$ is the piston work, $\partial Q_{comb}/\partial\theta$ is the rate of heat release by the fuel combustion, $\partial Q_w/\partial\theta$ is the rate of heat transfer through the cylinder walls, $h_{bb}dm_{bb}/d\theta$ is the energy lost due to blow-by (leakage of combustion gases that pass between the rings and the cylinder wall into the crankcase), $q_{vap}f dm_{vap}/d\theta$ represents the rate of energy consumption by the fuel vaporization. In Eq. (1), all the terms are given as rates with respect to the crankshaft angular position θ , measured in degrees. The rates $d(\cdot)/d\theta$ are easily converted to time rates $d(\cdot)/dt$, with time in seconds, by multiplying by 6ω degrees per second, where ω is the engine speed in *rpm* (rotations per minute).

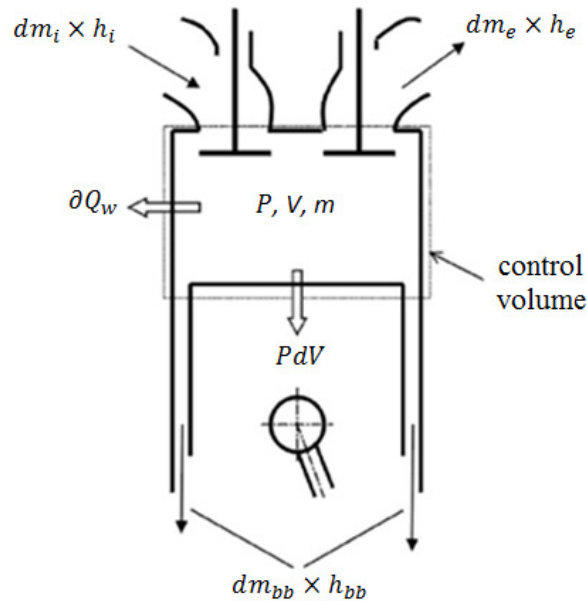


Figure 1. Energy balance in the cylinder (AVL, 2011a).

The rate at which energy is released by combustion is established by the combustion model adopted in the simulation. The choice is an important one, since the energy release interferes with the pressure, temperature, and heat transfer curves, and as a consequence, with the engine power.

2.1 Combustion model

The engine simulator offers the following options for the model of heat release by fuel combustion: *Wiebe*, *Double Wiebe*, *Table*, *Constant Volume*, *Constant Pressure*, *Fractal*, *Target Pressure Curve*. In the present work, the *Fractal* model has been chosen. This model is quasi-dimensional, and splits the air/fuel mixture region in two zones, the *burned zone* and the *unburned zone*.

The main reason for the choice of the *Fractal* model to simulate the combustion process is that, once the model parameters are adjusted for a given fuel and operational conditions, it is not necessary to readjust the parameters when a different fuel is used. Another important aspect of the model is that, it is capable of predicting the ignition delay and the combustion duration. These quantities are necessary when the behaviors of different burning fuels are being compared in a spark ignition ICE.

According to Carvalho *et al.* (2013), the *Fractal* model assumes that the flame front is an irregular surface that propagates with the speed of a laminar flame, and whose area can be described by a fractal geometry. This assumption is based on combustion visualization experiments, and has been validated by Dober and Watson (2000), Pajot *et al.* (2001) and Bozza *et al.* (2005). In the *Fractal* model the fuel burning rate, dm_b/dt , is modeled based on the flame propagation, which is proportional to the density of the unburned mixture, and is given by

$$\frac{dm_b}{dt} = \rho_u A_L S_T \quad (2)$$

where ρ_u is the density of the unburned mixture, A_L is the area of the laminar flame front, considered an spherical area centered at the spark plug location, and S_T is the flame characteristic turbulent velocity.

2.2 Heat transfer model

In global models for instantaneous heat transfer in internal combustion engines (ICE), it is common to employ Newton's law of cooling

$$Q_w = h_c A (T - T_w) \quad (3)$$

to calculate the heat transfer rate. Equation (3) relates the heat transfer rate Q_w with the difference between the wall temperature T_w and the gas temperature T through a convection heat transfer coefficient h_c , multiplied by the surface area A . The surface area for the instantaneous heat transfer encompasses the combustion chamber, piston, and cylinder surfaces of the engine.

The engine simulator *AVL Boost*TM makes available four options of heat transfer models to determine the convection coefficient (AVL, 2001b): *Woschni 1978*, *Woschni 1990*, *Hohemberg e AVL 2000*. Wu *et al.* (2006) verified the efficacy of the *Hohemberg* model for low-displacement motorcycle engines, obtaining good results. Hence, the *Hohemberg* model is used here, expressed by the equation

$$h_c = C_1 V^{-0,06} P^{0,8} T^{-0,4} (v_p + C_2)^{0,8} \quad (4)$$

where C_1 and C_2 are engine-adjusted constants, v_p is the piston speed, and V , P , and T are instantaneous volume, pressure and temperature, respectively, of the mixture of gases.

2.3 Friction model

The engine simulator *AVL Boost*TM offers three options of friction models (AVL, 2001b): *Table*, *PNH* (Patton, Nitschke and Heywood) e *SLM* (Shayler, Leong and Murphy). In the present work, as previously utilized in successful simulations with the *AVL Boost*TM (Carvalho *et al.*, 2010, 2013), the *PNH* model has been adopted. It requires as input data, information relative to the valves actuating system and the lubricant oil.

The *PNH* model was developed by Patton *et al.* (1989) based on fundamental scaling laws combined with the analysis of experimental results. The model calculates the friction mean effective pressure, *FMEP*, with the expression

$$FMEP = (FMEP_{cr} + FMEP_{pi} + FMEP_{val} + FMEP_{aux} + FMEP_{oil}) \left(\frac{v_{T_{oil}}}{v_{T_{oil}=90^{\circ}C}} \right)^{0,24} \quad (5)$$

where $FMEP_{cr}$, $FMEP_{pi}$, $FMEP_{val}$, $FMEP_{aux}$, and $FMEP_{oil}$ are the friction mean effective pressures related to the crankshaft, piston, valves actuating system, auxiliary losses, and oil injection pump, respectively. The last term on the right is due to the effect of the oil viscosity variation as a function of temperature. The equations for each component of *FMEP* are given in the article by Patton *et al.* (1989), and, for the sake of brevity, are not repeated here.

3. INPUT DATA

Since the fuels used in this work, gasoline E22 and hydrous ethanol (ANP, 2011a, 2011b), are not available in the *AVL Boost*TM database, it has been necessary to insert the volume fractions of the mixture components in the program field *General Species Setup*. Thus, the fuels used have been inserted as mixtures of the components gasoline, anhydrous ethanol fuel (AEF), and water, as shown in Tab. 1. The capital letter "H" indicates the percentage of hydrous ethanol fuel (HEF) in the mixture of gasoline E22 and HEF. Gasoline E22 contains 22% v/v of AEF. Water is considered to be present in the fuel mixture as liquid, because HEF has up to 4.9% v/v of water in its composition (ANP, 2011b).

R. Azevedo Cruz Neto, A.J.K. Leiroz and M.E.C. Cruz
Simulation of a Motorcycle Engine Operating with Gasoline and Ethanol Blends

Table 1. Volume fractions of each species in the fuel mixture.

Fuel Mixtures	Gasoline (%)	AEF (%)	Water (%)
H0 (Gasoline E22)	78.0000	21.9120	0.0880
H25	58.5000	40.2090	1.2910
H50	39.0000	58.5060	2.4940
H75	19.5000	76.8030	3.6970
H100 (HEF)	0.0000	95.1000	4.9000

To run an engine simulation with the program *AVL Boost*TM, dimensional data of the engine, such as compression ratio, piston bore and stroke, displacement volume, length and diameter of inlet and exhaust ducts, are also necessary. In addition, one needs to specify data related to the valve opening characteristic curve. All such data for the motorcycle engine of this study are presented in Tab. 2.

Table 2. Specifications of the motorcycle engine.

Engine type	Four-Stroke, Air Cooled, OHC
Bore x Stroke	57.30 x 57.84 mm
Fuel System	Electronic Injection
Number of valves	2
Displacement Volume	150 cc
Compression Ratio	9.5
Spark Advance	8°/1500 rpm, 29°/4500 rpm
Pipe Diameter	20.8 mm (Inlet) and 18 mm (Exhaust)
Pipe Length	236 mm (Inlet) and 953 mm (Exhaust)
Valve open timing (opened 1 mm)	2° BTDC (Inlet) and 27° BTDC (Exhaust)
Valve closed timing (opened 1 mm)	28° ATDC (Inlet) and 2° ATDC (Exhaust)
Maximum Valve Opened	4.9071 mm (Inlet) and 4.7938 mm (Exhaust)

4. MODEL VERIFICATION

To simulate the motorcycle engine with the flex-fuel technology as faithfully as possible, the *Fractal* model parameters have first been adjusted based on the experimental results for effective power. Data about effective power measured directly on the crankshaft for low-displacement motorcycle SI engines have not been found in the literature. Therefore, the data available in the work by Azevedo Cruz Neto *et al.* (2011) have been employed, who used the same engine considered here, and measured the power values on a vehicular dynamometer at the wheel shaft of the motorcycle. On the other hand, simulations with the program *AVL Boost*TM will calculate values for the power at the crankshaft. To effect the data estimation from wheel shaft power to crankshaft power, the methodology of the European Directive 2002/41 (2002) has been used. The Directive is based on the specification of mechanical efficiencies for several elements of the powertrain in two- or three-wheel vehicles.

Figure 2 shows the estimated values for the experimental crankshaft power Ne_{cr} , based on the measurements by Azevedo Cruz Neto *et al.* (2011), as well as the values for the simulated indicated power Ni and simulated effective power Ne obtained with the software *AVL Boost*TM. The simulations have been realized at full load conditions, which are compatible with the experiments. Henceforth, the value of 7500 rpm for the engine speed ω has been used in several investigations of the present work, since it is the value that corresponds to the maximum values of the crankshaft power Ne_{cr} and simulated indicated power Ni .

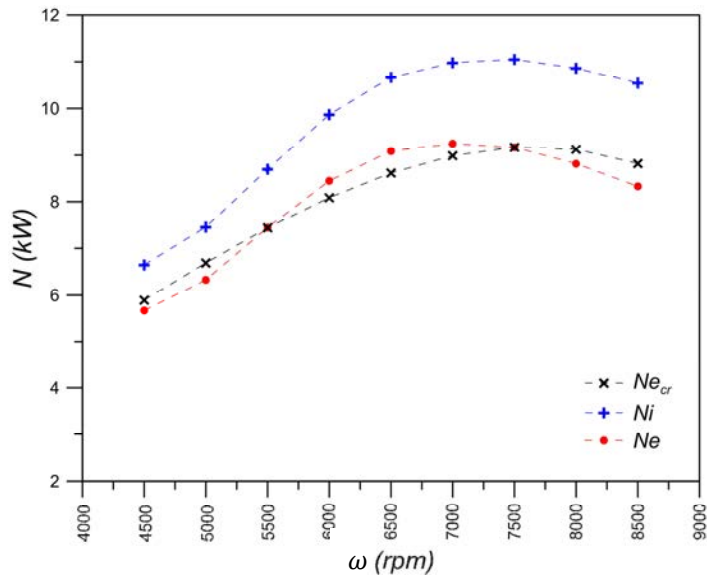


Figure 2. Simulated indicated power N_i and simulated effective power N_e obtained with the software *AVL Boost*TM, and estimated experimental crankshaft power $N_{e_{cr}}$ (Azevedo Cruz Neto *et al.*, 2011), for several values of engine speed ω (rpm) – H0.

5. RESULTS

In this section the results obtained with the simulations of the motorcycle engine using the *AVL Boost*TM are presented. The curves for pressure, mass, temperature, and heat transfer are shown for several mixtures of gasoline and ethanol, and selected engine speeds. All the engine simulations have been realized at full load conditions.

5.1 Mass inside the cylinder

The total mass intake during each cycle influences the amount of heat release by the fuel combustion, which in turn determines the maximum values of pressure and temperature reached inside the cylinder. Figure 3 presents the mass inside the cylinder versus the crankshaft angle for several mixtures of gasoline and ethanol, at the same value of engine speed (7500 rpm). The broken vertical lines indicate, from left to right, inlet valve closing (IVC), top dead center (TDC), and exhaust valve opening (EVO), respectively. The interval between IVC and EVO represents the closed phase of the cycle, with no mass flux through the valves.

The process of mass intake during a cycle can be visualized in Fig. 3. Mass increases inside the cylinder until a little before the IVC. The opposite behavior is seen after the EVO, when mass decreases inside the control volume along the exhaust process. It can be observed that at the locations close to zero degree (or 720 degrees) the value of the mass is a nonzero minimum, indicating the presence of residual gases of combustion. The residual gases influence the heating of the new air/fuel mixture which enters the cylinder, as well as the combustion process.

Figure 4 presents the curves for the mass inside the cylinder for different engine speeds. One can verify that the total entering air/fuel mass increases up to 6500 rpm, when it starts to decrease. This behavior is due to the fact that the injected fuel mass, and thus also the total mass, increases as the engine speed increases. However, the increase in engine speed causes a reduction in the engine volumetric efficiency. Thus at more elevated engine speeds, beyond 6500 rpm, the total mass intake is reduced. The back-flow at the inlet valve can also be detected in Fig. 4, through the peaks that are formed at lower engine speeds before the point IVC. The peaks are practically nonexistent at the more elevated engine speeds.

R. Azevedo Cruz Neto, A.J.K. Leiroz and M.E.C. Cruz
Simulation of a Motorcycle Engine Operating with Gasoline and Ethanol Blends

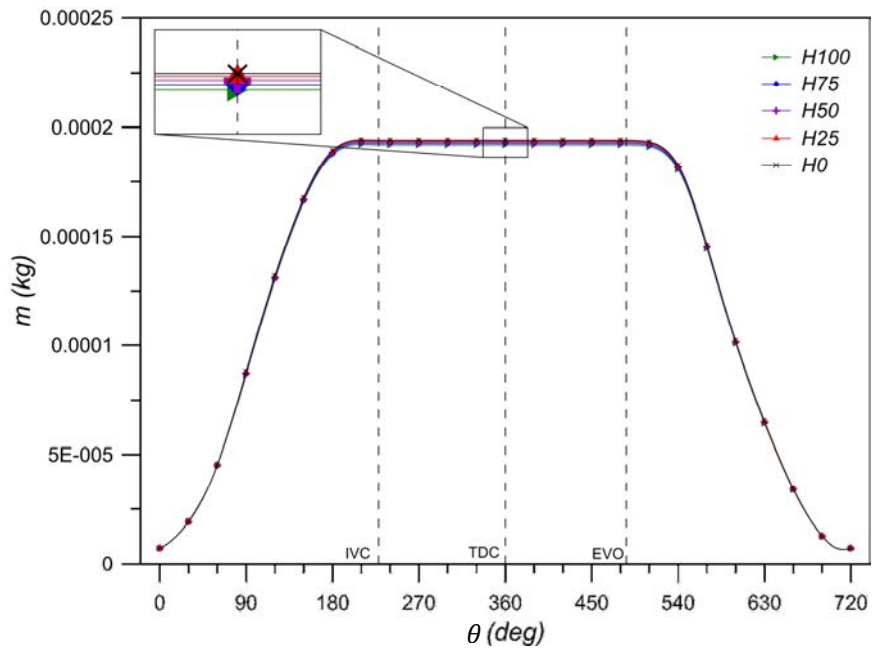


Figure 3. Mass m (kg) of the mixture of gases versus crankshaft angle θ (deg) for the mixtures H0, H25, H50, H75 and H100 – 7500 rpm.

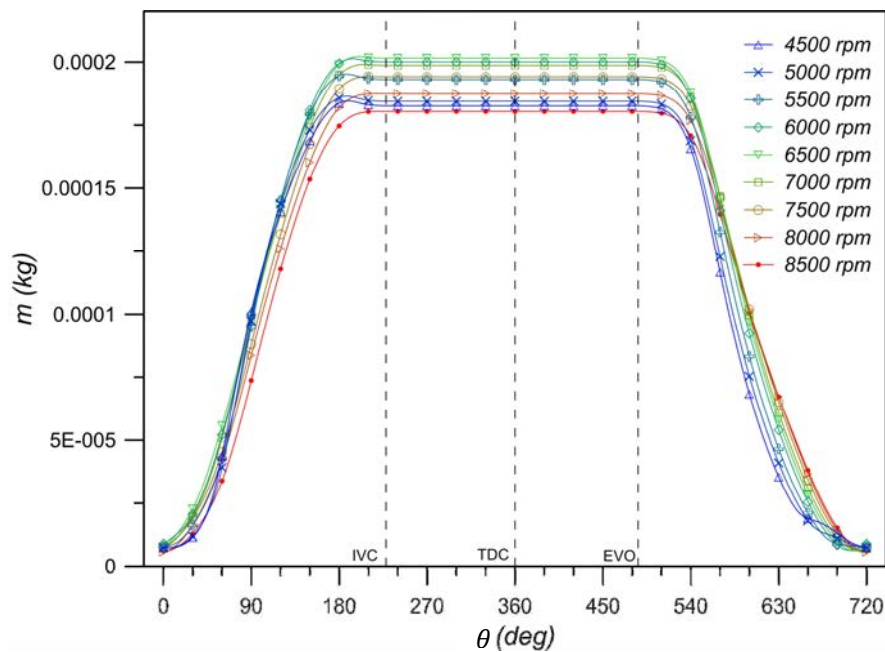


Figure 4. Mass m (kg) of the mixture of gases versus crankshaft angle θ (deg) for different engine speeds ω (rpm) – H0.

5.2 Pressure inside the cylinder

Figure 5 displays the pressure curves for the mixtures of gasoline and ethanol considered in the present work. One can verify that the values of maximum pressure are all very close, regardless of the percentage of hydrous ethanol in the mixture. In the present study, the similar peak pressures for all mixtures are probably due to the fact that the same spark advance has been used in all simulations.

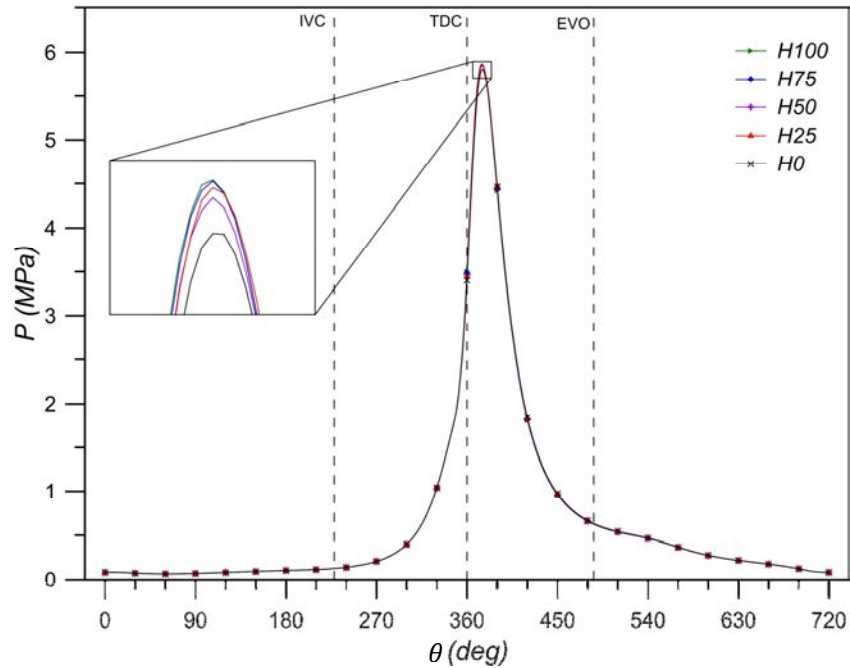


Figure 5. Instantaneous pressure of the mixture of gases P (MPa) versus crankshaft angle θ (deg) for H0, H25, H50, H75 and H100 – 7500 rpm.

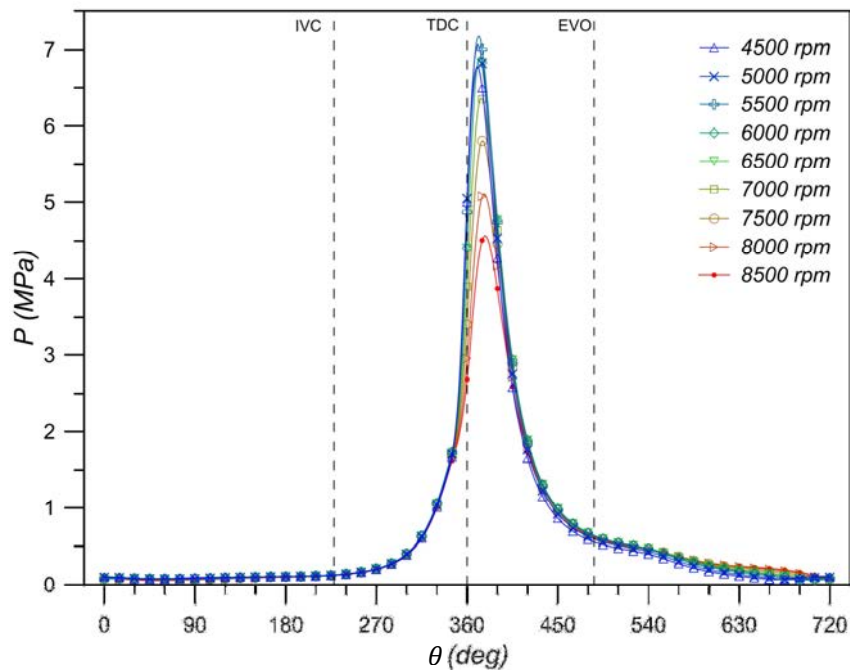


Figure 6. Instantaneous pressure of the mixture of gases P (MPa) versus crankshaft angle θ (deg) for different engine speeds ω (rpm) – H0.

In Fig. 6 the pressure peaks increase up to 5500 rpm. Beyond 5500 rpm, as the engine revolutions increase, the pressure peaks decrease. This behavior is due to two reasons, the variation of the total mass intake, which influences the heat released by combustion, and the increase in the duration of combustion, $\Delta\theta$, as the engine speed increases (Tab. 3). The increase in $\Delta\theta$ shifts the angle where the heat released is maximum. This angle, to the right of TDC, is indicated as $\theta_{50\%}$, and corresponds to the angle where half of the mixture has been burned. The angle $\theta_{50\%}$ can be visualized by the pressure peaks moving to the right of TDC as the engine speed increases.

Table 3. Duration of combustion, $\Delta\theta$, and $\theta_{50\%}$ for different engine speed ω (rpm) – H0.

ω (rpm)	$\Delta\theta$ (1 – 99%) (deg)	$\theta_{50\%}$ (deg)
4500	81.5	361.0
5000	85.5	362.5
5500	86.5	363.0
6000	87.5	364.0
6500	88.5	366.0
7000	92.5	368.0
7500	94.2	369.9
8000	100.0	373.0
8500	105.0	375.0

5.3 Heat transfer

Figure 7 presents the curves for heat transfer through the walls of the engine cylinder, Q_w , for the various gasoline and ethanol blends considered. It can be observed that the heat transfer is close to zero during the mixture inlet process, before the IVC, due to the temperature of the gases being close to the temperature of the walls of the cylinder. The heat transfer rates start to increase just before the TDC, during the compression process and due to the beginning of the combustion process. The maximum values are observed right after the TDC, during the expansion of the high temperature combustion gases. The maximum values of heat transfer are all close when the engine operates at the same engine speed, irrespective of the mixture burned.

In Fig. 8 it can be seen that, as the engine speed increases, the maximum values of heat transfer through the cylinder wall decrease. This behavior is explained by the fact that, as the engine speed increases, the time interval for the complete engine cycle (0 to 720 degrees) decreases and, therefore, the contact time between the gases and the cylinder walls is reduced.

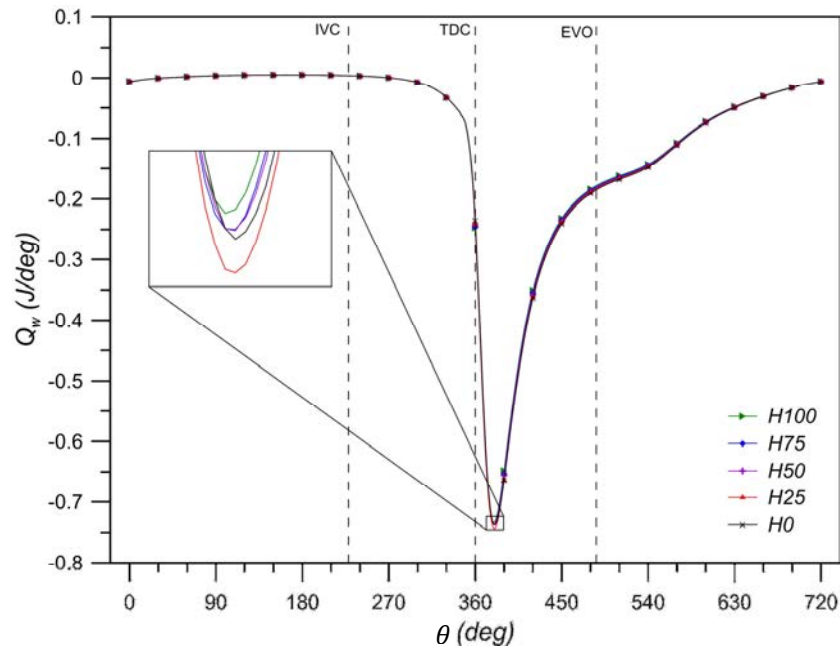


Figure 7. Rate of heat transfer Q_w (J/deg) between the mixture of gases and the cylinder walls versus the crankshaft angle θ (deg) for H0, H25, H50, H75 and H100 – 7500 rpm.

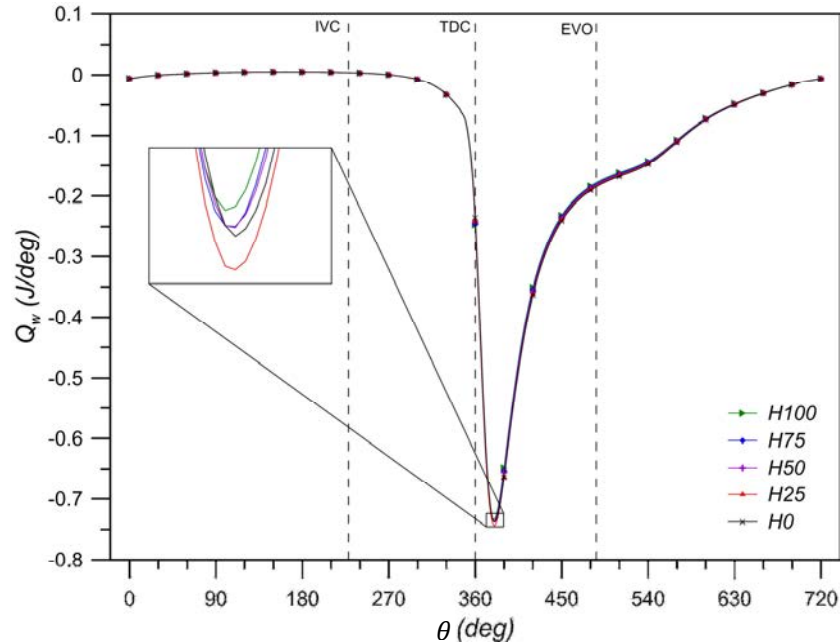


Figure 8. Rate of heat transfer Q_w (J/deg) between the mixture of gases and the cylinder walls versus the crankshaft angle θ (deg) for different engine speed ω (rpm) – H0.

5.4 Temperature inside the cylinder

In Fig. 9 the temperature curves for different mixtures of gasoline and ethanol are shown, for the same engine speed. It can be observed that the temperature values along the entire cycle are very similar for all mixtures. The values are slightly more elevated for mixtures with low hydrous ethanol content.

The temperature curves for different engine speeds can be visualized in Fig. 10. One can verify that, following the same trend as the heat transfer curves in Fig. 8, the temperature peaks decrease as the engine speed increases. The temperature of the exhaust gases after the EVO increases as the engine speed becomes more elevated.

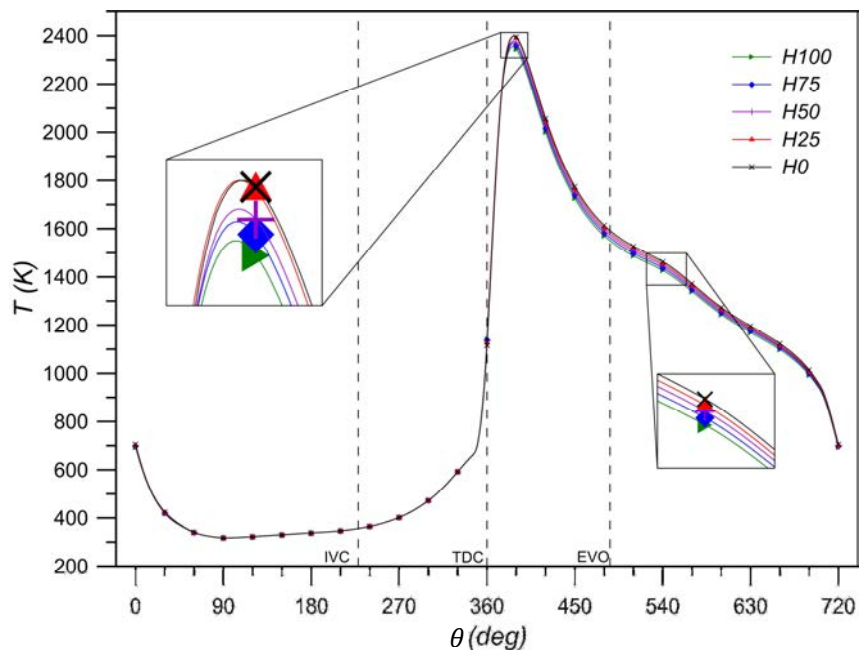


Figure 9. Instantaneous temperature T (K) of the mixture of gases versus crankshaft angle θ (deg) for H0, H25, H50, H75 and H100 – 7500 rpm.

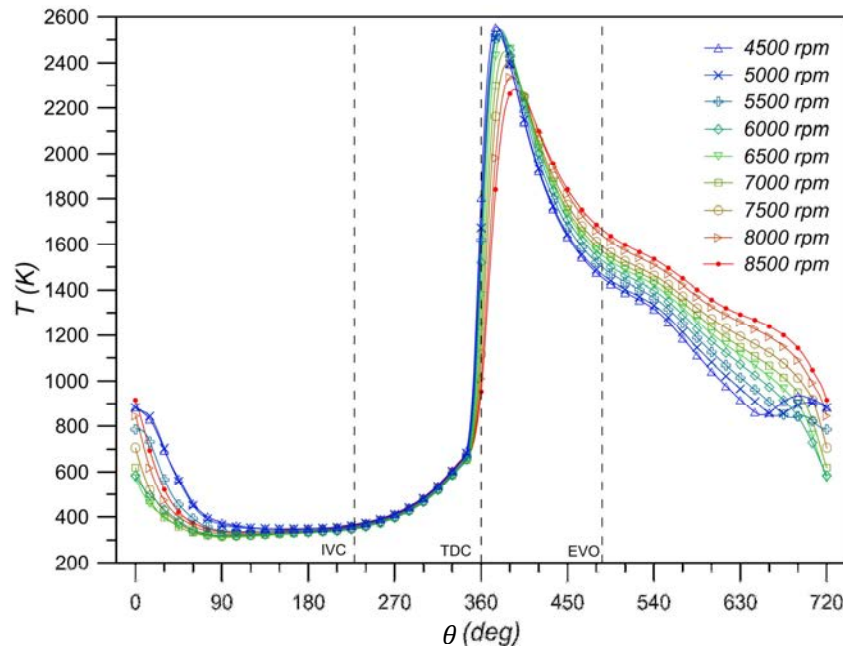


Figure 10. Instantaneous temperature T (K) of the mixture of gases versus crankshaft angle θ (deg) for different engine speed ω (rpm) – H0.

5.5 Engine energy efficiency

The engine energy efficiency values are shown in Tab. 4 for different engine speeds, and different mixtures of gasoline and ethanol. The efficiency is calculated based on the amount of energy contained in the fuel mass that enters the control volume, and the work done along one complete cycle (0 to 720 degrees). Both quantities are available in the simulations results obtained with the program *AVL Boost*TM. As the ethanol content in the mixture increases, the energy efficiency is seen to increase. This is a result of the fact that the maximum values for pressure and temperature are close, when the different mixtures are burned.

The maximum efficiency is seen to occur at 4500 rpm for all mixtures. The decrease in the energy efficiency values with the increase in the engine speed is due, mainly, to the reduction in the volumetric efficiency, and the increased separation of the pressure peaks relative to the TDC.

Table 4. Thermal efficiency η (%) for different engine speed ω (rpm), and different mixtures of gasoline and ethanol.

ω (rpm)	η (%)				
	H0	H25	H50	H75	H100
4500	34.55	34.95	35.34	35.66	36.10
5000	33.85	34.20	34.47	34.72	35.14
5500	33.68	33.80	34.05	34.35	34.68
6000	33.31	33.49	33.68	33.93	34.25
6500	32.93	33.12	33.19	33.42	33.70
7000	31.96	32.26	32.77	32.61	32.91
7500	31.01	31.26	31.30	31.54	31.81
8000	30.46	30.69	30.87	30.91	31.12
8500	29.15	29.38	29.61	29.76	30.06

6. CONCLUSIONS

In the present work, numerical simulations of a low-displacement motorcycle SI engine operating with gasoline and ethanol blends are successfully conducted, using the commercial code *AVL Boost*TM.

It has been observed that the values of pressure and temperature are all very close for all fuel mixtures simulated. The similar values for all mixtures are probably due to the fact, that the same spark advance has been used in all simulations, whereas in reality the spark advance is increased as more ethanol is present in the mixture. Because of the smaller lower heating value of ethanol and the similar values of pressure and temperature for all mixtures, the energy efficiency increases as the ethanol content in the mixture also increases. The study thus shows that hydrous ethanol rich mixtures are in fact a good option for low-displacement motorcycle engines with the flex-fuel technology.

Results also show a decrease on energetic efficiency when the engine speed is increased. This outcome is due to the reduction of volumetric efficiency and the dislocation of the pressure peak position away from the TDC.

It is suggested for future works that experiments be realized to obtain combustion data in motorcycle SI engines, such that computational simulations can be improved to generate more reliable results. Specifically, for low-displacement high-speed motorcycle engines operating with different fuel blends, it is suggested to obtain data for the combustion initiation and duration, pressure and temperature curves as functions of crankshaft angle, and molar composition of the exhaust gases.

7. ACKNOWLEDGEMENTS

R.M. Azevedo Cruz Neto is thankful to CAPES and FAPEAM for the research scholarship. M.E. Cruz thanks CNPq (Grant PQ-302725/2009-1) and FAPERJ (Grant CNE-E26/103.058/2011) for the continued support.

8. REFERENCES

- ANP - Agência Nacional do Petróleo, Gás Natural e Biocombustíveis, 2011a, Especificações para a comercialização da gasolina automotiva no Brasil, Resolução 57.
- ANP - Agência Nacional do Petróleo, Gás Natural e Biocombustíveis, 2011b, Especificações para a comercialização do álcool etílico hidratado combustível no Brasil, Resolução 7.
- AVL List GmbH, 2011a, BOOST – Theory, Graz, Austria.
- AVL List GmbH, 2011b, BOOST – User’s Guide, Graz, Austria.
- Azevedo Cruz Neto, R. M., Azevedo, J. D. L., Lopes, S. P., 2011, “Comparative performance of a motorcycle flex-fuel using different mixtures of ethanol and gasoline”, In: 21st Brazilian Congress of Mechanical Engineering, COBEM 2011, Natal, RN, Brazil, ISSN: 2176-5480.
- Azevedo Cruz Neto, R. M., 2013, “Simulação Computacional e Análise Exergética de um Motor de Motocicleta de Baixa Cilindrada com Misturas de Gasolina e Etanol”, Dissertação de Mestrado, PEM/COPPE, UFRJ, Rio de Janeiro, RJ, Brasil.
- Bozza, F., Gimelli, A., Merola, S. S., Vaglieco, B., 2005, “Validation of a fractal combustion model through flame imaging”, In: SAE World Congress, Detroit, MI, USA, SAE number 2005-01-1120.
- Carvalho, L. O., Cruz, M. E. C., Leiroz, A. J. K., 2010, “Integração de Simuladores de Processos e de Motores para a Análise Exergética de Plantas de Potência”, In: VI Congresso Nacional de Engenharia Mecânica, Campina Grande, PB, Brasil, Paper CON10-1096.
- Carvalho, L. O., Leiroz, A. J. K., Cruz, M. E., 2013, “Exergetic Analysis of Cogeneration Plants Through Integration of Internal Combustion Engine and Process Simulators”, Heat Transfer Engineering, vol. 34, nos. 5-6, pp. 520-531.
- Cordtz, R., Ivarsson, A., Schramm, J., 2011, “Steady State Investigation of DPF Soot Burn Rates and DPF Modeling”, In: 10th International Conference on Engines & Vehicles, SAE Technical Paper 2011-24-0181.
- Directive 2002/41/EC, 2002, “Adapting to technical progress Directive 95/1/EC of the European Parliament and of the Council on the maximum design speed, maximum torque and maximum net engine power of two- or three-wheel motor vehicles”.
- Dober, G. G., Watson, H. C., 2000, “Quasi-dimensional and CFD modeling of turbulent and chemical flame enhancement in an ultra lean burn S.I. engine”, In: SAE World Congress, Detroit, MI, USA, SAE number 2000-01-1263.
- Melo, T. C. C., 2012, “Análise Experimental e Simulação Computacional de um Motor Flex Operando com Diferentes Misturas de Etanol Hidratado na Gasolina”, Tese de Doutorado, PEM/COPPE, UFRJ, Rio de Janeiro, RJ, Brasil.
- Pajot, O., Mounaïm-Rousselle, C., Queiros-Conde, D., 2001, “New data on flame behaviour in lean burn SI engine”, In: International Spring Fuels and Lubricants, Orlando, FL, USA, SAE number 2001-01-1956.
- Patton, K. J., Nitschke, R. G., Heywood, J. B., 1989, “Development and evaluation of a friction model for spark-ignition engines”, In: SAE International Congress and Exposition, Detroit, MI, USA, Technical Paper 890836.
- Vicentini, P. C., 2011, “Uso de modelos de qualidade do ar para avaliação do efeito do PROCONVE entre 2008 e 2020 na região metropolitana do Rio de Janeiro”, Tese de Doutorado, PEM/COPPE, UFRJ, Rio de Janeiro, RJ, Brasil.

R. Azevedo Cruz Neto, A.J.K. Leiroz and M.E.C. Cruz
Simulation of a Motorcycle Engine Operating with Gasoline and Ethanol Blends

Wu, Y. Y., Chen, B. C., Hsieh, F. C., 2006, "Heat transfer model for small-scale air-cooled spark ignition four-stroke engines", *Int. J. Heat Mass Transfer*, vol. 49, no. 21–22, pp. 3895–3905.

Teng, H., 2011, "A Thermodynamic Model for a Single Cylinder Engine with Its Intake/Exhaust Systems Simulating a Turbo-Charged V8 Diesel Engine", In: *SAE 2011 World Congress & Exhibition*, SAE Technical Paper 2011-01-1149.

Tuan, L. A., Truyen, P. H., Khanh, N. D., Chuan, T. T., 2011, "Simulation Study of Motorcycle Engine's Characteristics Fueled with Ethanol-Gasoline Blends", *Journal of Science & Technology*, No. 83B, pp. 119-124.

9. RESPONSIBILITY NOTICE

The authors are the only responsible for the printed material included in this paper.